UNITU-THEP-4/1996 May 28, 1996
(revised) in press by Nucl. Phys. A

A renormalizable extension of the NJL-model*

K. Langfeld, C. Kettner[1], H. Reinhardt

Institut für theoretische Physik, Universität Tübingen
D–72076 Tübingen, Germany.

Abstract

The Nambu-Jona-Lasinio model is supplemented by the quark interaction generated by the one-gluon exchange. The employed gluon propagator exhibits the correct large momentum behavior of QCD, whereas the Landau-pole at low energies is screened. The emerging constituent quark model is one-loop renormalizable and interpolates between the phenomenologically successful Nambu-Jona-Lasinio model (modified by a transversal projector) at low energies and perturbative QCD at high momenta. Consequently, the momentum dependence of the quark self-energy at high energy coincides with the prediction from perturbative QCD. The chiral phase transition is studied in dependence on the low energy four quark interaction strength in the Dyson-Schwinger equation approach. The critical exponents of the quark self-energy and the quark condensate are obtained. The latter exponent deviates from the NJL-result. Pion properties are addressed by means of the Bethe-Salpeter equation. The validity of the Gell-Mann-Oakes-Renner relation is verified. Finally, we study the conditions under which the Nambu-Jona-Lasinio model is a decent approximation to our renormalizable theory as well as the shortcoming of the NJL-model due to its inherent non-renormalizability.

* Supported in part by DFG under contract Re 856/1-3.

[1] Supported by "Graduiertenkolleg: Hadronen und Kerne"

1 Introduction

Most striking evidence for Quantumchromodynamics (QCD) as the right theory of strong interactions stems from high energy scattering experiments [1], where experiments confirm the theoretical predictions. The remarkable property of asymptotic freedom implies that the running parameters of the theory, e.g. coupling constant and current masses, decrease with the inverse logarithm of the energy scale to the power of the corresponding anomalous dimension [1], allowing a perturbative treatment. At low energies, the effective coupling constant becomes large and even diverges at the so-called Landau pole which occurs at the typical energy scale of QCD Λ_{QCD}. It was recently argued [2], that the Landau pole is an artifact of the assumption of a perturbative vacuum, and that non-perturbative physics, which sets in at low energies scales, screens the Landau singularity. Since non-perturbative QCD is not yet under control, this implies that for a description of low-energy hadron physics one has to resort to effective models.

Low-energy hadron physics is dominated by the approximate chiral symmetry embodied by QCD [3]. In their pioneering work, Nambu and Jona-Lasinio proposed an effective theory with chirally invariant four fermion interaction [4], and illuminated the mechanism of spontaneous breaking of chiral symmetry, which led to a successful description of the light pseudo-scalar mesons as Goldstone bosons. The simple handling of the model allows for a wide range of applications describing the light mesons [10] and baryons [11]. Recently, the model was also extended to describe heavy hadrons [12].

Although the original version of Nambu and Jona-Lasinio was invented to describe nucleons and their interactions, the re-interpretation of the model with quarks as fundamental particles gained further importance, when it was realized that the low-energy effective quark theory of QCD should be of NJL type. This idea is supported in particular by the instanton picture [5] and the field strength approach to QCD [6, 7]. In the context of strong coupling QED, it was argued that the so-called "irrelevant" four fermion interaction of the effective theory becomes relevant due to a large anomalous dimension [8]. It was further observed that a NJL-type fermion interaction naturally arises in the dual formulation of strongly coupled scalar QED [9]. These field theoretical investigations indicate that an effective quark model should exhibit a NJL-type interaction in the low energy regime.

Despite the wide spread success of the NJL-model, it suffers from two shortcomings, i.e. the absence of quark confinement, which e.g. allows for a decay of the heavy mesons into free quarks, and its non-renormalizability. The latter enforces that the interaction is cut off at some momentum scale, which defines the range of applicability of the model. As a consequence, processes involving large momentum structure, e.g. form-factors at high momenta and anomalous decays like $\pi \to \gamma\gamma$, cannot be adequately described by the model. Physics which involve the interaction at high

momentum can be properly described in the one-gluon exchange models [13, 14, 15], which match the correct high energy behavior of QCD.

The confining mechanism of QCD is still an unresolved problem. In certain super-symmetric Yang-Mills theories, it became apparent that the condensation of monopoles plays a key role [16]. Unfortunately, a concise understanding of confinement in QCD is not available at the moment. At the level of an effective quark theory, an extension of the NJL-model was proposed which realizes confinement by random background fields [17]. In the context of the one-gluon exchange models, confinement is described by a quark propagator which vanishes due to infra-red singularities [14], or which does not have poles corresponding to asymptotic quark states [15]. In this paper, we will not address the question of confinement at the level of effective theories, but focus on the consequences of renormalizability[1].

Here we propose an effective quark model which in the low energy regime coincides with the NJL-model modified by a transversal projector (see equation (2)), and which matches the well known perturbative quark interaction at high energies at an energy scale Λ_I. We naturally choose $\Lambda_I > \Lambda_{QCD}$ in order that the NJL-part of the interaction screens the unphysical Landau pole. Since the interaction strength of the NJL-interaction is fixed by the constraint to match the interaction induced by the one-gluon exchange at high energies, the only parameter of our model is Λ_I.

Our model should not be mixed up with the gauged NJL-model [8, 18, 19]. In the latter, the NJL-interaction exists over the whole momentum range in addition to the gauge interactions. This model is non-perturbatively renormalizable and represents an interesting alternative to the standard mechanism of electro-weak symmetry breaking [20]. It is, however, not suitable in the context of the standard formulation of QCD. This is because its effective quark interaction does not reduce to the one-gluon exchange at high energies.

The organization of the paper is as follows: In the next section, our model is defined, and its renormalization is discussed at the level of the Dyson-Schwinger equation. To this aim, the high-energy behavior of the quark self-energy is investigated by solving the Dyson-Schwinger equation numerically as well as analytically, using the Landau approximation in the latter case. Furthermore, the dependence of the chiral phase transition on the low energy four quark interaction strength is studied in some detail. In section 3, pion physics is addressed by means of the Bethe-Salpeter equation. The Gell-Mann-Oakes-Renner relation is established. Numerical results concerning pion properties are presented. Finally, we compare our model with the standard NJL-model in section 4. In particular, the shortcomings of the latter model due to its non-renormalizability are discussed. A summary and conclusions are left to the last section. Some explicit calculations are given in three

[1] At the moment, there is little empirical evidence that confinement is important in hadron-physics at energy scales below the would-be quark thresholds.

appendices.

2 Model description and renormalization

2.1 Model building

For the description of hadrons we propose an effective one-gluon exchange model which is defined by the following generating functional (in Euclidean Space)

$$\begin{aligned} Z[\phi] &= \int \mathcal{D}q\mathcal{D}\bar{q}\, \exp\{-\left[S - \int d^4x\, \bar{q}(x)\phi(x)q(x)\right] , \qquad (1) \\ S &= \int d^4x\, \bar{q}(i\partial\!\!\!/ + im)q + \frac{1}{2}\int d^4x d^4y\, \bar{q}(x)t^a\gamma_\mu q(x)\mathcal{D}^{ab}_{\mu\nu}(x-y)\bar{q}(y)t^b\gamma_\nu q(y) , \end{aligned}$$

where m is the bare current quark mass, t^a, $a = 1 \ldots 8$ are the generators of SU(3) color group and γ_μ are the Hermitian Dirac matrices. Furthermore, $\phi(x)$ is an external meson source. For $m = 0$, the model is chiral invariant. The interaction is diagonal in color space, $\mathcal{D}^{ab}_{\mu\nu} = \delta^{ab}D_{\mu\nu}$, and consists of two parts, which, in momentum space, are separated by an energy scale Λ_I, i.e.

$$D_{\mu\nu}(k) = \left[G\,\theta(\Lambda_I - |k|) + \frac{4\pi\alpha(k^2)}{k^2}\theta(|k| - \Lambda_I)\right]\left(\delta_{\mu\nu} - \frac{k_\mu k_\nu}{k^2}\right) , \qquad (2)$$

where $\theta(x)$ is the step function and $|\cdot|$ denotes the module at a Euclidean 4-vector. Choosing

$$\alpha(k^2) = \frac{12\pi}{(33 - 2N_f)\ln k^2/\Lambda^2_{QCD}} , \qquad (3)$$

where N_f is the number of quark flavors, the second term in (2) represents for $k > \Lambda_I$ the perturbative gluon propagator of QCD multiplied by the effective (running) coupling constant $\alpha(k^2)$. The coupling strength G of the NJL-term is chosen to match the gluonic interaction at the scale Λ_I, i.e.

$$G = \frac{4\pi\,\alpha(\Lambda_I^2)}{\Lambda_I^2} . \qquad (4)$$

In order to study the spontaneous breakdown of chiral symmetry, we investigate the quark self-energy $\Sigma(p)$. It can be obtained from the Dyson-Schwinger equation, which in ladder approximation reads

$$-i\not{p} + m + \frac{4}{3}\int \frac{d^4k}{(2\pi)^4}\,\gamma_\mu\, S(k+p)\,\gamma_\nu\, D_{\mu\nu}(k) = S^{-1}(p) . \qquad (5)$$

Here

$$S(p) = \frac{i}{Z(p^2)\not{p} + i\Sigma(p)} . \qquad (6)$$

is the quark propagator, which is diagonal in color space, and we have used $\sum_{a,l} t^a_{il} t^a_{lk} = \frac{4}{3}\,\delta_{ik}$. It will turn out (see section 2.3) that the loop integration in (5) is in fact ultra-violet finite, since the gluon propagator decreases like $1/k^2\,\ln(k^2/\Lambda^2_{QCD})$ for large values of k^2, and the self-consistent solution $\Sigma(k^2)$ is asymptotically proportional to $1/[\ln k^2/\mu^2]^{d_m}$, where $d_m = 4/9$ is the anomalous mass dimension for three quark flavors. In addition, no finite renormalization constants are needed in (5), because the freedom in the functions $Z(p^2)$ and $\Sigma(p^2)$ is sufficient to accomplish for the standard renormalization conditions of the quark propagator.

Using the ansatz (6), the Dyson-Schwinger equation can be cast into two equations which determine the self-energy $\Sigma(p^2)$ and the quark wave-function $Z(p^2)$, i.e.

$$\begin{aligned}
\Sigma(p^2) &= m + 4G \int_{|k|<\Lambda_I} \frac{d^4k}{(2\pi)^4}\, \frac{\Sigma((p+k)^2)}{Z^2((p+k)^2)(p+k)^2 + \Sigma^2((p+k)^2)} \qquad (7)\\
&+ 4 \int_{|k|>\Lambda_I} \frac{d^4k}{(2\pi)^4}\, \frac{\Sigma((p+k)^2)}{Z^2((p+k)^2)(p+k)^2 + \Sigma^2((p+k)^2)}\, \frac{4\pi\alpha(k^2)}{k^2}\,,\\
Z(p^2) &= 1 + \frac{4G}{3} \int_{|k|<\Lambda_I} \frac{d^4k}{(2\pi)^4}\, \frac{Z((p+k)^2)}{Z^2((p+k)^2)(p+k)^2 + \Sigma^2} \left(1 + 3\frac{p\cdot k}{p^2} + 2\frac{(p\cdot k)^2}{k^2p^2}\right)\\
&+ \frac{4}{3} \int_{|k|>\Lambda_I} \frac{d^4k}{(2\pi)^4}\, \frac{Z((p+k)^2)}{Z^2((p+k)^2)(p+k)^2 + \Sigma^2} \left(1 + 3\frac{p\cdot k}{p^2} + 2\frac{(p\cdot k)^2}{k^2p^2}\right)\\
&\times \frac{4\pi\alpha(k^2)}{k^2}\,. \qquad (8)
\end{aligned}$$

Note, that the k-integration never crosses the Landau singularity at $|k| = \Lambda_{QCD}$ due to our assumption $\Lambda_I > \Lambda_{QCD}$.

2.2 Numerical results

To pave the ground for later investigations, we first present a numerical solution of the Dyson-Schwinger equation in the chiral limit $m \equiv 0$ and discuss its relevant properties. The numerical method to solve the system of coupled differential equations as well as the procedure to estimate the numerical errors are described in some detail in appendix A.

The actual choice of the fundamental energy scale Λ_{QCD} depends on the regularization scheme, which is used to extract the divergent parts. In the $\overline{MS}$-scheme, which employs dimensional regularization, its typical value is $\Lambda_{QCD} \approx 100 \ldots 200\,\mathrm{MeV}$ [1], whereas in the one-gluon exchange models, which generically use a sharp O(4)-invariant cutoff (and therefore a momentum-subtraction scheme), values up to 500 MeV are consistent with phenomenology [13, 14]. In the case of the present model, it will turn out that the choice $\Lambda_{QCD} = 500\,\mathrm{MeV}$ reproduces the experimental data for the static pion properties (see section 3). For illustrative

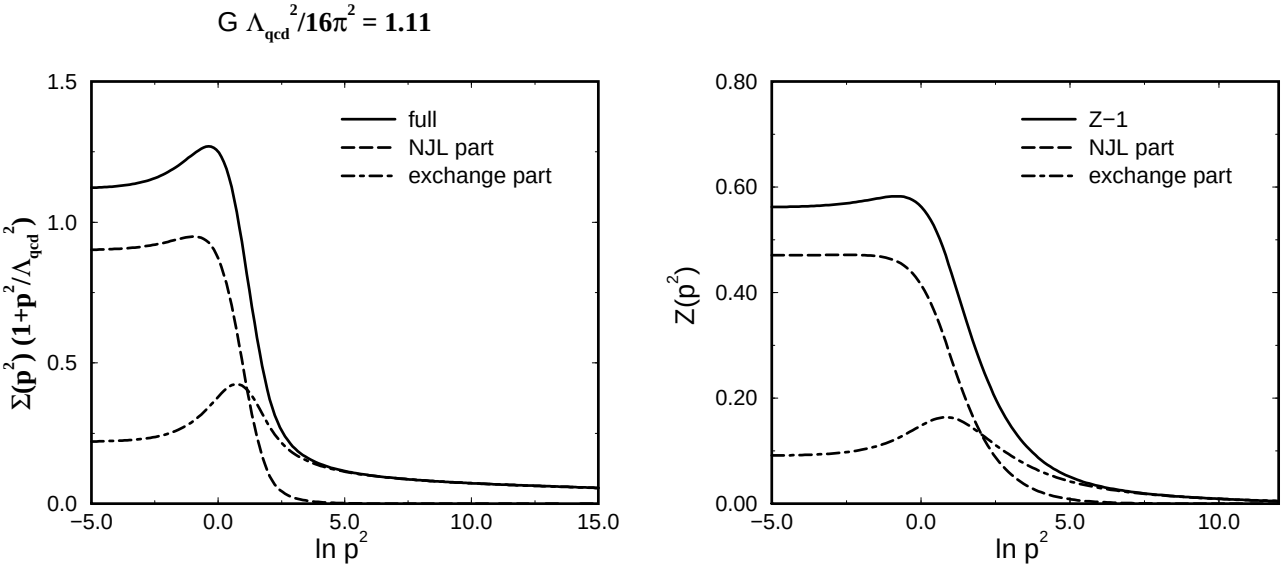

Figure 1: The self-energy $\Sigma(p^2)$ times $1 + p^2/\Lambda_{QCD}^2$ in units of Λ_{QCD} and the wave function $Z(p^2)$ as function of the momentum transfer p^2 (full lines). Also shown are the contributions from the NJL part of the interaction (long dashed) and from the gluon exchange term (dot-dashed).

purposes, let us choose $G = 1.11\ 16\pi^2/\Lambda_{QCD}^2$. It will turn out, that this choice for G is to small to provide a constituent quark mass of $M \approx 310\,\mathrm{MeV}$.

The numerical result for the self-energy $\Sigma(p^2)$ and the wave function $Z(p^2)$ for three flavors ($N_f = 3$) is shown in figure 1. Although both integrals in (7) are equally important in order to calculate the self-consistent solution $\Sigma(p^2)$, it is instructive to split $\Sigma(p^2)$ into the contributions stemming from the NJL type interaction (first line in (7)) and from the one-gluon exchange term *after* the self-consistent solution was obtained. These contributions are also plotted in figure 1. As expected, the NJL term dominates at small momentum transfer, whereas the high momentum behavior is exclusively determined by the one-gluon exchange part of the interaction.

The high-momentum behavior of the quark constituent mass function, i.e.

$$M(p^2) \ := \ \frac{\Sigma(p^2)}{Z(p^2)}\,, \tag{9}$$

is of particular interest, since it can be compared with the result from perturbative QCD. Including the leading operator-product corrections, the mass function is

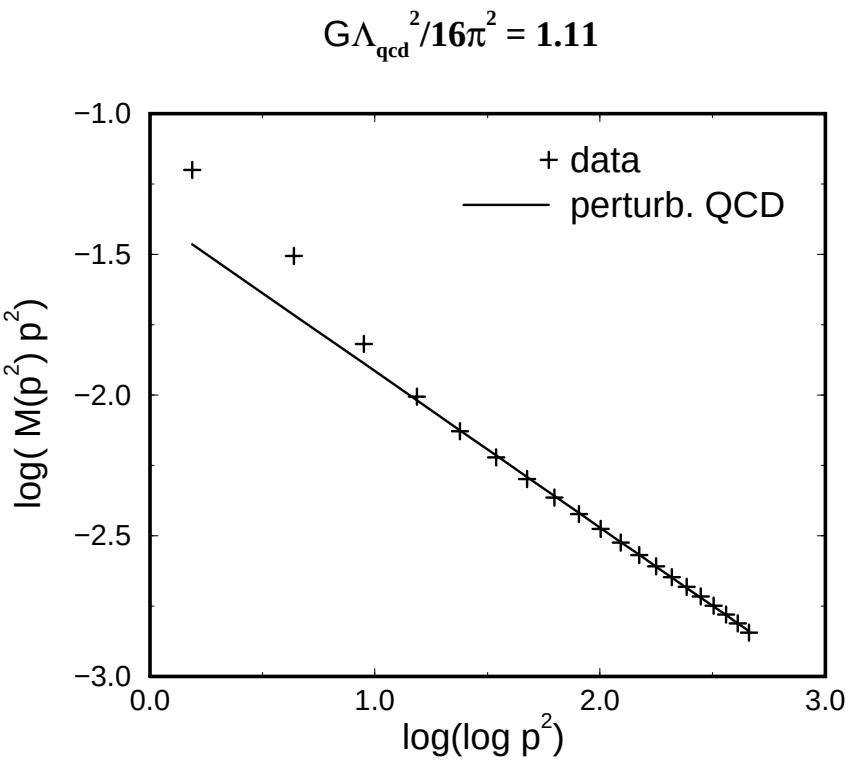

Figure 2: The asymptotic behavior of the quark mass function $M(p^2)$ (points) compared with the result of perturbative QCD (line).

asymptotically (for large values of p^2) given by [21],

$$M(p^2) \approx \frac{m_R(\mu)\left[\ln(\mu^2/\Lambda^2_{QCD})\right]^{d_m}}{\left[\ln(p^2/\Lambda^2_{QCD})\right]^{d_m}} - \frac{4\pi^2 d_m}{3p^2}\frac{\langle\bar{q}q\rangle(\mu)\left[\ln(\mu^2/\Lambda^2_{QCD})\right]^{-d_m}}{\left[\ln(p^2/\Lambda^2_{QCD})\right]^{1-d_m}} + \cdots \quad (10)$$

where m_R and $\langle\bar{q}q\rangle$ is the renormalized current mass and the quark condensate, respectively, at a renormalization point μ, and d_m is the anomalous dimension of the current mass. In perturbative QCD one finds [1, 21]

$$d_m \;=\; \frac{12}{33-2N_f} \;=\; \frac{4}{9} \qquad \text{for} \qquad N_f = 3\,. \quad (11)$$

In the chiral limit, the mass function $M(p^2)$ asymptotically decreases like $1/p^2$ with logarithmic corrections. The same is true for the self-energy $\Sigma(p^2)$, since the wave function $Z(p^2)$ logarithmically approaches 1. Figure 2 exhibits the asymptotic behavior of the numerical result for $M(p^2)$. The numerical data show a logarithmic decrease of $p^2\,M(p^2)$. The line corresponds to an anomalous dimension of the quark condensate of $1 - d_m = 5/9$, which agrees with the result of perturbative QCD [1].

2.3 Analytical results

The asymptotic behavior of the quark mass function (10) is well known from perturbative QCD studies augmented with OPE corrections [21]. In the following we will show that our model Dyson-Schwinger equation (7,8) yields a quark self-energy $\Sigma(p^2)$ which has the correct asymptotic (large p^2) behavior predicted by QCD. The asymptotic form of Dyson-Schwinger equations was studied in detail for many models. For a review we refer to the book of Miransky [22].

In the case of our model, we firstly show that the NJL part of the integral equation (7) does not affect the asymptotic behavior of $\Sigma(p^2)$, as it was already observed in the numerical calculation (see figure 1). In fact, since the momentum integration in the NJL-term is over a finite volume in momentum space, the integrand can be expanded in powers of k^2/Λ_I^2. Obviously, this contribution to $\Sigma(p^2)$ is suppressed by powers of Λ_I^2/p^2, i.e.

$$\Sigma(p^2) \;=\; \frac{G}{8\pi^2}\,\frac{\Lambda_I^4}{Z^2(p^2)p^2}\,\Sigma(p^2) \;+\; \ldots\;, \tag{12}$$

implying that asymptotically ($p^2 \to \infty$) only the gluon exchange term contributes.

In appendix B we show that in the Landau approximation[2] and for non-vanishing renormalized current mass the coupled set of Dyson-Schwinger equations (7,8) has for $p^2 \to \infty$ the asymptotic solution

$$\Sigma(p^2) \;\approx\; \frac{\kappa}{\left[\ln \frac{p^2}{\Lambda_{QCD}^2}\right]^{\alpha}}\;, \tag{13}$$

where

$$\alpha \;=\; \frac{12}{33-2N_f} \;=\; d_m\;, \tag{14}$$

and κ is proportional to the renormalized current mass m_R. Furthermore, the bare current mass runs with the cutoff as

$$m(\Lambda_{UV}) \;=\; \frac{\kappa}{[\ln \Lambda_{UV}^2/\Lambda_{QCD}^2]^{\alpha}}\;, \qquad \kappa \;=\; m_R(\mu)\left[\ln(\mu^2/\Lambda_{QCD}^2)\right]^{d_m}\;. \tag{15}$$

In the chiral limit ($m_R = 0$), the asymptotic solution is given by

$$\Sigma(p^2) \;\approx\; \frac{c}{p^2\left[\ln \frac{p^2}{\Lambda_{QCD}^2}\right]^{\beta}}\;, \qquad \beta \;=\; 1-d_m\;, \tag{16}$$

where c is measure for the quark condensate (compare with equation (10)).

The main observation in this subsection is that the large momentum behavior of the solutions $\Sigma(p^2)$, $Z(p^2)$ of the coupled set (7,8) of differential equations agrees with the QCD predictions.

[2] This approximation is only applied in this subsection. The numerical studies in this paper treat the full Dyson-Schwinger equations (7,8)

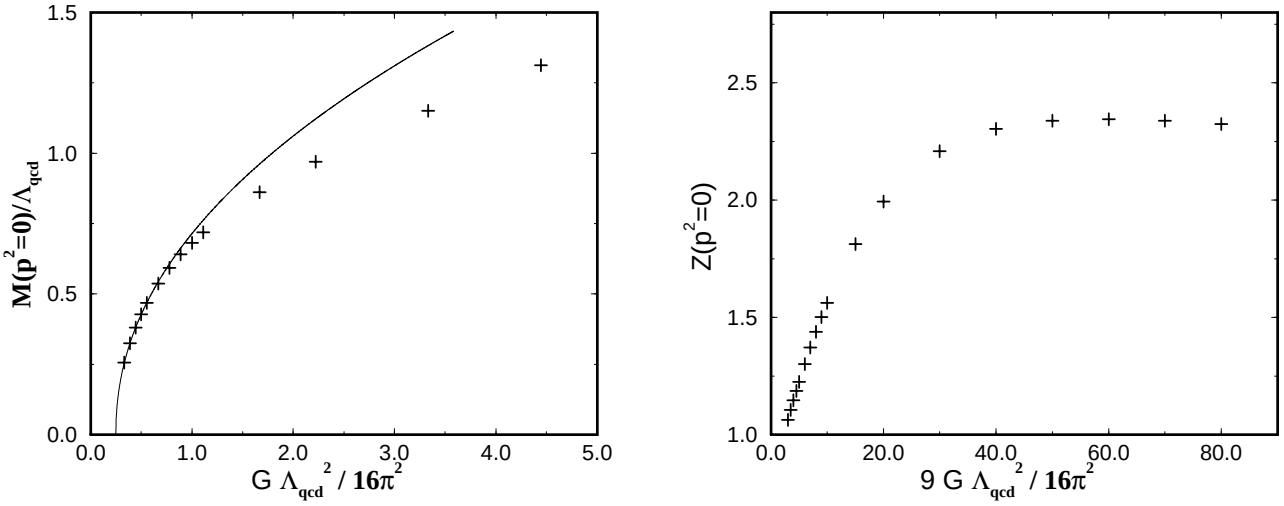

Figure 3: The quark mass function $M(p^2 = 0)$ (crosses) and $Z(p^2 = 0)$ (crosses) at zero momentum transfer as function of the coupling strength G of the low energy effective four quark interaction. Also shown is the fit (solid line) according (18).

2.4 Chiral phase transition

The results found in the previous subsection, i.e. a non-vanishing quark self-energy with the correct decrease at asymptotic large values of the momentum transfer, establishes that chiral symmetry is spontaneously broken for an appropriate choice of parameters ($G > G_c$). Here, we will report details of the chiral phase transition at the critical value G_c of the effective four quark interaction. We have numerically investigated the quark self-energy $\Sigma(p^2 = 0)$ and the wave function $Z(p^2 = 0)$ at zero momentum transfer by solving the coupled set of integral equations (7) and (8) for various values of G, the only parameter[3] which is not fixed by perturbative QCD results. The results are depicted in figure 3. For small values of $G < G_c$, the chiral symmetry is not spontaneously broken and $\Sigma(p^2) = 0$ is the only solution to equations (7,8). However, if the coupling exceeds the critical value[4]

$$G_c \approx \Big(0.26 \pm 0.011\Big) \times \frac{16\pi^2}{\Lambda_{QCD}^2}\,, \tag{17}$$

a non-trivial self-energy signals the spontaneous breakdown of chiral symmetry. For values G slightly above the critical coupling G_c, our numerical results are well fitted

[3] Note that Λ_I is fixed by the constraint (4).

[4] The procedure to obtain an estimate of the numerical error is discussed in appendix A.

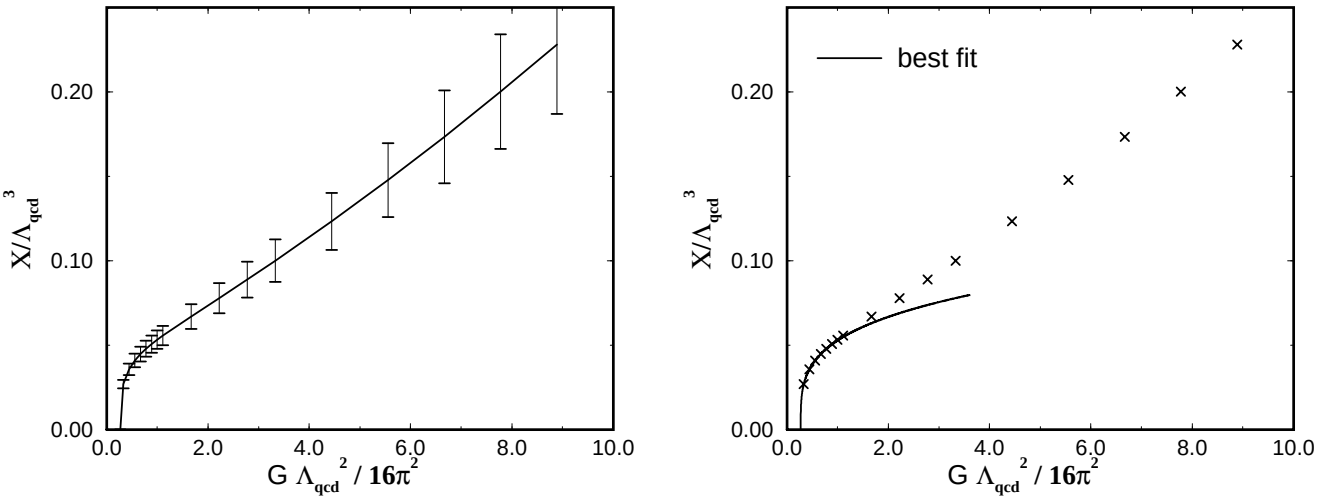

Figure 4: The quark condensate $\chi = -\langle\bar{q}q\rangle$ at a renormalization point $\mu = 1\,\mathrm{GeV}$ as function of the low energy interaction strength G. The solid line in the right hand picture is the fit function (20).

by

$$M(p^2 = 0) \;\approx\; 0.43\,\Lambda_{QCD}\,\left(\frac{G}{G_c} - 1\right)^{\delta_\Sigma} \qquad \delta_\Sigma \;=\; 0.47\,. \tag{18}$$

If $\epsilon = G/G_c - 1$ measures the deviation of the coupling strength from its critical value, the behavior of the order parameter close to the phase transition is in general $M \approx \epsilon^\delta$, where the critical exponent is characteristic of the underlying field theory only [25]. In our case (18), a critical exponent of $1/2$ is compatible with the numerical data.

Figure 3 also shows the wave function $Z(p^2 = 0)$ as function of G. For $G < G_c$, the wave function takes its canonical value $Z(p^2 = 0) = 1$. For values G larger than the critical coupling G_c, the function $Z(p^2 = 0)$ linearly increases with increasing strength G. It saturates, and becomes a constant independent of G for sufficiently large G.

Finally, we present the quark condensate as a function of the interaction strength G. The quark condensate at a renormalization point μ is defined via the trace of the quark propagator $S(k)$ (6) (see subsection 3.2), i.e.

$$\langle\bar{q}q\rangle(\mu) \;=\; -\left[\ln\frac{\mu^2}{\Lambda^2_{QCD}}\right]^{d_m}\left[\ln\frac{\Lambda^2_{UV}}{\Lambda^2_{QCD}}\right]^{-d_m}\int_{k^2<\Lambda_{UV}}\frac{d^4k}{(2\pi)^4}\,\mathrm{tr}\,S(k)\,. \tag{19}$$

It was shown in [26] that this definition of the quark condensate is compatible with the definition via the asymptotic behavior of the mass function (10), which is used in the operator product expansion (see also subsection 3.2). The numerical result of the quark condensate at a renormalization point of $\mu = 1\,\mathrm{GeV}$ is shown in figure 4. For values G close to G_c, the numerical data is well represented by the function

$$\langle\bar{q}q\rangle(\mu = 1\,\mathrm{GeV}) \;\approx\; -0.041\;\Lambda_{QCD}^3\;\left(\frac{G}{G_c} - 1\right)^{\delta_\chi}\;, \quad \text{with} \quad \delta_\chi \approx 0.27\;. \tag{20}$$

In the standard NJL-model, the quark condensate is directly proportional to the self-energy implying that this model yields a critical exponent of 1/2. This simple connection between the self-energy and the condensate is artificial, since the condensate is in general a subject of renormalization. In particular, the critical exponent of our model significantly deviates from 1/2.

3 Static pion properties

3.1 The Bethe-Salpeter equation

In the constituent quark picture, the pion is described as a pseudo-scalar bound state of a quark anti-quark pair. This bound state is characterized by its vertex function $P(p,q)$, which satisfies a Bethe-Salpeter (BS) equation. The momentum p thereby represents the four momentum of the pion, and q reflects the internal structure of the pion. In our case, the BS-equation is

$$P(p,q) \;=\; \int_k i\gamma_\mu\; t^a\; D_{\mu\nu}(k-q)\; S(k+p/2)\; P(p,k)\; S(k-p/2)\; t^a\; i\gamma_\nu\;, \tag{21}$$

where $D_{\mu\nu}(k-p)$ is the effective interaction (2) of our model.

In the following, we will solve this equation (21) within a derivative expansion. This expansion was earlier obtained in references [23] and [24]. For later use, we briefly re-derive the expansion in our notation.

For this purpose, first note that the BS-equation (21) can be formally written as an eigenvalue equation, i.e.

$$P_p \;=\; \int_q K(\Sigma, p^2, k, q)\; P_p(q) \quad \text{or:} \quad P_p = K(\Sigma, p) P_p\;, \tag{22}$$

where the BS-vertex P_p is represented as a vector, and the kernel $K(\Sigma, p)$ depends on the self-energy $\Sigma(k^2)$ and the pion momentum p. For later convenience, we introduce a "scalar product" of two vectors a and b via a quark loop integral, i.e.

$$\langle a \,|\, b\rangle := \mathrm{tr} \int \frac{d^4k}{(2\pi)^4}\; S_0(k - \frac{p}{2})\; a^\dagger(k - \frac{p}{2}, k + \frac{p}{2})\; S_0(k + \frac{p}{2})\; b(k + \frac{p}{2}, k - \frac{p}{2})\;. \tag{23}$$

As a warm-up exercise, we show that the pion BS-vertex is given in the chiral limit by

$$P_0(k^2) \;=\; \frac{\sqrt{2}}{f_\pi}\,\gamma_5\,\Sigma_0(k^2)\;, \tag{24}$$

where Σ_0 is the self-energy in the chiral limit, and f_π is the pion decay constant. The relation (24) is a particular case of the general relation between the BS-equation at zero energy and the Schwinger-Dyson equation. From (6), one has that $S_0(k)\gamma_5 S_0(k) = \gamma_5(Z_0^2(k^2)k^2 + \Sigma_0^2(k^2))^{-1}$. A direct calculation then yields

$$K(\Sigma_0, p^2=0)\;P_0 \;=\; P_0\;, \tag{25}$$

where the Dyson-Schwinger equation (5) was used. P_0 (24) indeed describes a pseudo-scalar quark anti-quark bound state with zero mass, i.e $m_\pi^2 = -p^2 = 0$. The normalization of the BS-vertex is not fixed by the linear equation (22). It can be related to the pion-decay constant by assuming that the axial-vector quark anti-quark coupling is entirely dominated by the axial-vector pion coupling in the chiral limit [15].

We now consider the case of a small explicit breaking of the chiral symmetry by the current mass m_R. In order to calculate the pion mass treating the explicit chiral symmetry breaking as a perturbation, we expand the BS-equation (22) to first order[5] in $p^2 = -m_\pi^2$ and m_R, i.e.

$$\Big[K(\Sigma_0, p=0) \;+\; K'(\Sigma_0, p=0)\;p^2 \;+\delta K\Big]\,(P_0 \;+\; \delta P) \;=\; (P_0 \;+\; \delta P)\;, \tag{26}$$

where K' denotes the derivative of K with respect to p^2, and
$\delta K := K(\Sigma, p=0) - K(\Sigma_0, p=0)$. The change in the pion mass in first order perturbation theory obtained by sandwiching equation (26) with $P_0^\dagger$. The contributions containing δP drop out as a consequence of the BS-equation in the chiral limit, and we are left with

$$0 \;=\; -\langle P_0\,|\,K'(\Sigma_0,0)P_0\rangle\;m_\pi^2 \;+\; \langle P_0\,|\,\delta K P_0\rangle\;. \tag{27}$$

In order to evaluate the second term at the right hand side of (27), one uses

$$\begin{aligned}&(K(\Sigma,0) \;-\; K(\Sigma_0,0))P_0 = \\ &\frac{\sqrt{2}}{f_\pi}\int\frac{d^4k}{(2\pi)^4}\;i\gamma_\mu t^a D_{\mu\nu}(k-q)\,[S(k)S(-k) \;-\; S_0(k)S_0(-k)]\,\Sigma_0(k)\gamma_5 t^a i\gamma_\nu\end{aligned}$$

to obtain finally

$$\langle P_0\,|\,\delta K P_0\rangle \;=\; \frac{8N_c}{f_\pi^2}\int\frac{d^4k}{(2\pi)^4}\;\Sigma_0^2(k^2)\frac{k^2(Z_0^2-Z^2)+\Sigma_0^2-\Sigma^2}{(Z^2k^2 \;+\; \Sigma^2)(Z_0^2k^2 \;+\; \Sigma_0^2)}\;. \tag{28}$$

[5]Note that current algebra shows that m_π^2 is of order m_R, which is also assumed in chiral perturbation theory.

The first term at the right hand side of (27) is more involved. This term explicitly reads

$$\langle P_0 \,|\, K'(\Sigma_0,0) P_0\rangle \;=\; \langle P_0 \frac{dK(\Sigma_0,p^2)}{dp^2}\Big|_{p^2=0} P_0\rangle \;=\; \frac{2}{f_\pi^2}\;\times \tag{29}$$

$$\mathrm{tr}\int_{q,k} t^a i\gamma_\nu S(q)\gamma_5\Sigma_0(q)S(q)i\gamma_\mu t^a D_{\mu\nu}(q-k)\;\frac{d}{dp^2}\left(S(k_+)\Sigma_0(k)\gamma_5 S(k_-)\right)\Big|_{p^2=0}\;,$$

where $k_\pm := k \pm p/2$. Inserting the BS-equation for the vertex function in the chiral limit, one gets rid of the double integration in (29), i.e.

$$\begin{aligned}\langle P_0 K'(\Sigma_0,0) P_0\rangle_0 \;&=\; \frac{2}{f_\pi^2}\frac{d}{dp^2}\left(tr\int_k \gamma_5\Sigma_0(k)S_0(k_+)\gamma_5\Sigma_0(k)S_0(k_-)\right)\Big|_{p^2=0} \\ &=\; -1\;.\end{aligned} \tag{30}$$

The last equality was obtained with the help of equation (76) of appendix C. Inserting (28) and (30) into (27), we obtain the mass formula

$$f_\pi^2\; m_\pi^2 \;=\; 8N_c\int\frac{d^4k}{(2\pi)^4}\;\Sigma_0^2(k^2)\frac{k^2(Z^2-Z_0^2)+\Sigma^2-\Sigma_0^2}{(Z^2k^2\;+\;\Sigma^2)(Z_0^2k^2\;+\;\Sigma_0^2)}\;. \tag{31}$$

This mass formula agrees with the result found earlier in reference [23] (see also [24]).

3.2 The Gell-Mann-Oakes-Renner relation

Since the momentum integration at the right hand side of (31) is rapidly converging, one is tempted to conclude that the GMOR relation, i.e.

$$f_\pi^2\, m_\pi^2 \;=\; -2m\,\langle\bar{q}q\rangle\;, \tag{32}$$

does not hold in the context of the one-gluon-exchange models, because the right hand side of (32) involves a divergent quark condensate whereas the left hand side is finite [23]. The apparent contradiction can be resolved by taking into account that the bare current mass m tends to zero for a large UV-cutoff (see (15)) implying that the product of bare mass and condensate might be finite.

The crucial quantity is the quark condensate which is defined via the trace of the quark propagator, i.e.

$$\langle\bar{q}q\rangle \;=\; -\frac{N_c}{4\pi^2}\;\int_0^{\Lambda_{UV}} dk^2\;k^2\;\frac{\Sigma(k^2)}{Z^2(k^2)+\Sigma^2(k^2)}\;. \tag{33}$$

In order to show that the condensate in (33) is divergent in the chiral limit $m_R(\mu)\equiv 0$, one uses the asymptotic behavior of the self-energy (10) and the fact that $Z(k^2)$ decreases to approach 1, yielding

$$\langle\bar{q}q\rangle \;=\; \langle\bar{q}q\rangle(\mu)\left[\ln(\mu^2/\Lambda_{QCD}^2)\right]^{-d_m}\;\left[\ln(\Lambda_{UV}^2/\Lambda_{QCD}^2)\right]^{d_m}\;+\;\text{finite terms}\;. \tag{34}$$

The crucial observation is that multiplying this divergent condensate with the bare current mass (see (15)) results in the finite value

$$m(\Lambda_{UV})\,\langle\bar{q}q\rangle \;=\; m_R(\mu)\,\langle\bar{q}q\rangle(\mu)\;. \tag{35}$$

To establish the GMOR relation (32), it remains to show that this finite value coincides up to a factor of 2 with the right hand side of the pion mass formula (31). This equivalence was first observed in [26] using the approximation $Z_0 \approx Z$. Below, we will generalize the results of [26]. For this purpose, we rewrite the DS-equation for the self-energy in the form

$$\Sigma(p^2) \;=\; m(\Lambda_{UV}) \;+\; 4\int_{k^2<\Lambda_{UV}} \frac{d^4k}{(2\pi)^4}\;\frac{\Sigma(k^2)}{Z^2k^2+\Sigma^2}\;d((p-k)^2)\;, \tag{36}$$

where $d(k^2) = D_{\mu\mu}(k^2)/3$. For later convenience, we also introduce the DS-equation for the self-energy Σ_0 in the chiral limit, i.e.

$$\Sigma_0(p^2) \;=\; 4\int_{k^2<\Lambda_{UV}} \frac{d^4k}{(2\pi)^4}\;\frac{\Sigma_0(k^2)}{Z_0^2k^2+\Sigma_0^2}\;d((p-k)^2)\;, \tag{37}$$

In order to estimate the change of the self-energy due to the presence of the bare mass, we subtract (37) from (36), i.e.

$$\Sigma(p^2)-\Sigma_0(p^2) = m(\Lambda_{UV})+4\int_{k^2<\Lambda_{UV}} \frac{d^4k}{(2\pi)^4}\;\left[\frac{\Sigma(k^2)}{Z^2k^2+\Sigma^2}-\frac{\Sigma_0(k^2)}{Z_0^2k^2+\Sigma_0^2}\right]\;d((p-k)^2)\;. \tag{38}$$

We then multiply both sides of this equation with

$$\frac{\Sigma_0(p^2)}{Z_0^2(p^2)p^2 \;+\; \Sigma_0(p^2)}$$

and integrate over the momentum p. Using the DS-equation (37), the result can be cast into the form

$$\begin{aligned}\int_{p^2<\Lambda_{UV}} \frac{d^4p}{(2\pi)^4}\,\Sigma_0(p^2)\,\frac{\Sigma(p^2)-\Sigma_0(p^2)}{Z_0^2p^2+\Sigma_0^2(p^2)} &= m(\Lambda_{UV})\int_{p^2<\Lambda_{UV}} \frac{d^4p}{(2\pi)^4}\;\frac{\Sigma_0(p^2)}{Z_0^2p^2+\Sigma_0^2(p^2)}\\ +\;\int_{k^2<\Lambda_{UV}} \frac{d^4k}{(2\pi)^4}\,\Sigma_0(k^2)\,&\left[\frac{\Sigma(k^2)}{Z^2k^2+\Sigma^2}-\frac{\Sigma_0(k^2)}{Z_0^2k^2+\Sigma_0^2}\right]\;.\end{aligned} \tag{39}$$

We therefore obtain the identity

$$\begin{aligned}\int_{k^2<\Lambda_{UV}} \frac{d^4k}{(2\pi)^4}\qquad &\Sigma_0(k^2)\,\Sigma(k^2)\left[\frac{1}{Z^2k^2+\Sigma^2}-\frac{1}{Z_0^2k^2+\Sigma_0^2}\right]\\ &=\; m(\Lambda_{UV})\int_{p^2<\Lambda_{UV}} \frac{d^4p}{(2\pi)^4}\;\frac{\Sigma_0(p^2)}{Z_0^2p^2+\Sigma_0^2(p^2)}\;.\end{aligned} \tag{40}$$

In the product $\Sigma_0\,\Sigma$, one might replace the Σ by the self-energy Σ_0 in the chiral limit, since the error is of higher order in the current mass m_R. Inserting then (40) into the right hand side of the pion mass formula (31) reproduces the GMOR relation (32), which completes the proof. Recently, the GMOR relation was also shown to hold true in effective one-gluon exchange models models which employ a running bare current mass [27].

3.3 Numerical results

In the table below, we finally present numerical results for the pion decay constant f_π, pion mass m_π and the quark condensate for five different values of the four quark coupling strength G. We also provide the results for the constituent quark mass M_c, which is defined by the pole of the constituent quark propagator, i.e.

$$p^2 \;=\; M(p^2)\,|_{p^2=M_c^2}\;, \tag{41}$$

where $M(p^2)$ is the mass function (9).

$\frac{G\Lambda_{QCD}^2}{16\pi^2}$	M_c	$[-\langle\bar{q}q\rangle(\mu=1\,\mathrm{GeV})]^{1/3}$	f_π	m_π
1.11	200 MeV	191 MeV	78 MeV	131 MeV
1.67	259 MeV	203 MeV	86 MeV	130 MeV
2.22	312 MeV	214 MeV	93 MeV	130 MeV
2.78	362 MeV	223 MeV	99 MeV	130 MeV
3.33	409 MeV	232 MeV	105 MeV	130 MeV

In these calculations, $\Lambda_{QCD} \approx 500\,\mathrm{MeV}$ was used, and $[m_u + m_d](\mu = 1\,\mathrm{GeV}) = 15\,\mathrm{MeV}$ for up- and down-quark masses was assumed. The values in the table should be compared with experimental ones, i.e. $f_\pi^{(exp)} = 93\,\mathrm{MeV}$ and $m_\pi^{(exp)} = 135\,\mathrm{MeV}$. The constituent quark mass is assumed to be approximately $m_N/3 \approx 310\,\mathrm{MeV}$, where m_N is the nucleon mass. It is remarkable that the pion mass nearly stays constant when G varies.

4 How effective is the NJL-model ?

In this section, we establish a direct relation between our renormalizable model and the familiar NJL-model [10]. In particular, we investigate the limits of the standard NJL-model [4] due to its non-renormalizability. For this purpose, we will search for a parameter range for which our model approximately reduces to the NJL-model. Then we study the accuracy of this approximation in comparison to a more realistic choice of parameters which reproduce the phenomenological data.

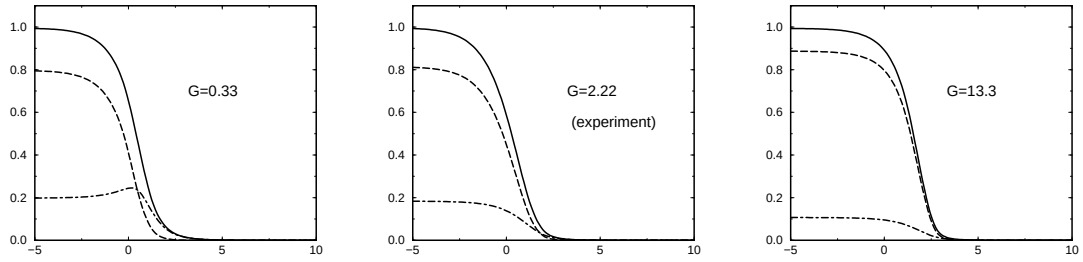

Figure 5: The contribution of the NJL-term (dashed) and the contribution from the non-local term (dash-dotted) to the self-energy (full) as function of $\ln p^2/\Lambda_{QCD}^2$ for various values of G in units of $16\pi^2/\Lambda_I^2$. The results are rescaled to ensure $\Sigma(0) = 1$.

The effective four quark interaction of our model consists of a NJL-type contact interaction at low momentum transfer $k < \Lambda_I$ and reproduces the effective perturbative one-gluon exchange at large momenta (see (2)). Consequently, the self-energy determined by the Dyson-Schwinger equation (7) receives two contributions. The first term coincides (up to the momentum dependence of the self-energy and to the presence of $Z(k^2)$) with the one obtained from the NJL gap equation, while the second term arises from the one-gluon-exchange. The self-consistent solution to the equations for $\Sigma(k^2)$ and $Z(k^2)$ in (7) and (8), respectively, (see figure 1) show that these functions are almost constant for $k < \Lambda_I$, and rapidly decrease at $k \approx \Lambda_I$ to approach the correct asymptotic behavior of Σ as dictated by perturbative QCD. We search for a parameter range, where the second term on the right hand side of the DS-equation (8) only yields a small contribution compared with the first term. In this range, we can expect that observables which are insensitive to large loop momenta are well described by the NJL-model. The numerical analysis shows that such a parameter range indeed exists (see figure 5). In the limit of a large effective four quark interaction G, the contribution to the self-energy from the non-local term is small. In this case, the approximately constant self-energy can be obtained from the reduced DS-equation (8), i.e.

$$\Sigma(0) \;\approx\; 4G \int_{|k|<\Lambda_I} \frac{d^4k}{(2\pi)^4} \; \frac{\Sigma(0)}{Z^2(0)k^2 + \Sigma^2(0)} \; . \tag{42}$$

This equation can be cast into the gap-equation of the NJL-model, i.e.

$$M \;=\; 4G_{NJL} \int_{|k|<\Lambda_{NJL}} \frac{d^4k}{(2\pi)^4} \; \frac{M}{k^2 + M^2} \; , \tag{43}$$

where

$$M \;=\; \frac{\Sigma(0)}{Z(0)}\,, \qquad G_{NJL} \;=\; \frac{G}{Z^2}\,, \qquad \Lambda_{NJL} \;=\; \Lambda_I \;\approx\; 500\,\mathrm{MeV}\,. \tag{44}$$

We therefore expect that observables involving rapidly converging loop integrals can be well estimated within the NJL-model, since the numerical value should be insensitive to the large momentum behavior. Such an observable is e.g. the pion decay constant defined in equation (77) of appendix C.

On the other hand, the NJL-model must fail for observables which receive considerable contributions from large momenta of the loop integrals. Here, we mention the anomalous decays of the pion as an example. In ref. [28], it was shown that the rate of the decay of the neutral pion into two photons, i.e.

$$\Gamma_{\pi^0\gamma\gamma} \;=\; \frac{m_\pi^3}{16\pi}\left(\frac{\alpha_{em}}{\pi f_\pi}\right)^2 g\,, \tag{45}$$

can be calculated in the chiral limit independently of the details of the quark-propagator, i.e.

$$g \;=\; \int_0^{\Lambda_{UV}^2\to\infty} dk^2\,\frac{\frac{d}{dk^2}C}{(1+C(k^2))^3} \;=\; \int_0^\infty dC\frac{1}{(1+C)^3} \;=\; \frac{1}{2}\,, \tag{46}$$

where $C(k^2) := \Sigma^2(k^2)/(k^2Z^2(k^2))$. The agreement of the theoretical prediction with the experimental value $g^{exp} = 0.504$ is very good and supports the constituent quark picture of hadrons. Since the formula (46) is independent of the details of the model, it is straightforward to apply it to the case of the NJL-model. In this case, the momentum integration in (46) is cutoff at Λ_{NJL}, and $C(k^2) = M^2/k^2$. One obtains[6]

$$g \;=\; \int_0^{\Lambda_{NJL}^2} dk^2\,\frac{\frac{d}{dk^2}C}{(1+C(k^2))^3} \;=\; \int_{M^2/\Lambda_{NJL}^2}^\infty dC\frac{1}{(1+C)^3} \;=\; \frac{1}{2}\,\frac{1}{1+\frac{M^2}{\Lambda_{NJL}^2}}\,. \tag{47}$$

The typical value of the ratio of constituent quark mass and NJL-cutoff is of order $M/\Lambda_{NJL} \approx 1/2$ implying that in the NJL-model the g-factor is underestimated by 20%.

The phenomenological data (see the table in the previous section) require an interaction strength $G \approx 2.22 \times 16\pi^2/\Lambda_I^2$. For this value, the NJL-term contributes 82% to the full self-energy. This result suggests that hadronic observables calculated within a NJL-model, where Λ_{NJL} is tightly related to the interaction strength G_{NJL}

[6] This result holds for an O(4) invariant sharp cutoff. Different regularization prescriptions might lead to different values g.

by (4), should deviate from the corresponding results obtained by a renormalizable model by approximately 18%. This is indeed the typical accuracy of the predictions of the NJL-model [10].

Finally, we mention that the NJL-propagator which arises as a limit of our renormalizable model possesses the structure

$$S_{NJL}(k) \;=\; \frac{i}{Z\,\not{k} \;+\; i\Sigma}\;, \qquad \text{with} \qquad Z \approx 2.3 \tag{48}$$

(despite of the generic form of the gap equation (43)). In the standard NJL-model, the Z-factor is independent of the momentum and set to 1 in order to obtain the generic residuum of the quark propagator. On the other hand in renormalizable models, the Z-factor depends, in principle, on the interaction strength. Fortunately, our numerical calculations have shown (see figure 3) that Z is approximately constant for sufficiently large coupling strength G, which is the parameter region where our model can be approximately reduced to an NJL-model. Therefore our investigations suggest a NJL-model with a momentum cutoff (see equation (44)), .i.e. $\Lambda_{NJL} = \Lambda_I \approx 500\,\mathrm{MeV}$. This value is in fact slightly smaller than the typical value, which arises from the fit of pion data within the NJL-model when pseudo-scalar axial-vector meson mixing is disregarded [10].

5 Summary and conclusions

We have proposed an effective quark theory which can be regarded as an (one loop) renormalizable extension of the phenomenologically successful NJL-model. The effective quark interaction of this model is given by a NJL-contact interaction at low momentum transfer ($k \leq \Lambda_I$), and is mediated by the one-gluon exchange augmented by the logarithmic QCD corrections at high energies, i.e.

$$D_{\mu\nu}(k) \;=\; \left[G\,\theta(\Lambda_I - |k|) \;+\; \frac{4\pi\alpha(k^2)}{k^2}\theta(|k| - \Lambda_I)\right]\left(\delta_{\mu\nu} - \frac{k_\mu k_\nu}{k^2}\right)\;,$$

where

$$G \;=\; \frac{4\pi\alpha(\Lambda_I^2)}{\Lambda_I^2}\;,\; \alpha(k^2) \;=\; \frac{12\pi}{(33-2N_f)\ln k^2/\Lambda_{QCD}^2}\;.$$

The intermediate energy scale Λ_I at which the low energy interaction matches the high energy one gluon exchange, is fixed by the choice of G. We demand $\Lambda_I > \Lambda_{QCD}$ in order to account for the screening of the Landau pole [2]. The model is (at least) one loop renormalizable. The numerical and analytical study of the asymptotic behavior of the quark self-energy $\Sigma(k^2)$ has yielded the correct anomalous dimensions for the current mass and quark condensate, which are know from perturbative QCD

calculations. A chiral phase transition from the perturbative chirally symmetric phase to a non-trivial chirally broken phase characterized by a non-vanishing quark condensate was found at sufficiently strong interactions, i.e. for

$$G \;>\; G_c \approx \Big(0.26 \pm 0.011\Big)\, \frac{16\pi^2}{\Lambda_{QCD}^2}\,.$$

The numerical data for the quark mass function and the quark condensate for an interaction strength G close to the critical one, G_c, are well fitted by

$$\begin{aligned} M(p^2=0) &\approx 0.43\,\Lambda_{QCD}\,\left(\frac{G}{G_c}-1\right)^{0.47}\,, \\ -\langle\bar{q}q\rangle(\mu = 1\,\mathrm{GeV}) &\approx 0.041\,\Lambda_{QCD}^3\,\left(\frac{G}{G_c}-1\right)^{0.27}\,. \end{aligned}$$

The critical exponent for the self-energy is consistent with $1/2$, whereas the exponent of the quark condensate significantly deviates form $1/2$.

Within our model, the emergence of the pion as a Goldstone boson was studied. The Bethe-Salpeter equation for the pion vertex was solved using a derivative expansion. We have analytically verified the Gell-Mann-Oakes-Renner relation (32), which relates the product of pion mass and decay constant to the product of current mass and condensate.

We have also established the relation of our model with the familiar NJL-model thereby exhibiting the limits of the latter due to its non-renormalizability. Like the NJL-model, our model does not contain quark confinement. We believe, however, that quark confinement is not of much relevance for low-energy hadron dynamics (if the external momenta are much smaller than the quark thresholds). On the other hand, renormalizability seems to be much more important, in particular, for processes which are sensitive to large loop momenta as e.g. the anomalous decay of the neutral pion. Our model is obviously superior to the NJL-model in these cases.

A Numerics

1. Solving the Dyson-Schwinger equation

In order to solve the coupled set of Dyson-Schwinger equations (7,8), the integration over the angle (between the vectors p and k) and over the loop momentum k must be done numerically. For this purpose, we have discretized the momentum at n points in logarithmic steps and used a cubic spline interpolation for the self-energy $\Sigma(k^2)$ and the quark wave-function $Z(k^2)$. The coupled set of differential equations is then solved by iteration. We used $n = 20$ and $n = 30$. It turned out that $n = 20$ is sufficient for most of the applications. For numerical reasons, the momentum

integration is cut off at $\Lambda_{UV}^2 = 3.3 \times 10^6 \Lambda_{QCD}^2$. By using also $\Lambda_{UV}^2 = 6.6 \times 10^7 \Lambda_{QCD}^2$, we have checked that our results are practically independent of the numerical cutoff. Since the functions Σ and Z depend on $(p+k)^2$, the numerical program needs an evaluation of this functions up to twice the numerical cutoff. Since the functions are only available for momenta smaller than Λ^{UV}, we used

$$\{Z,\, \Sigma\}(k^2) \;=\; \{Z,\, \Sigma\}(\Lambda_{UV}^2) \qquad \text{for} \qquad k^2 > \Lambda_{UV}^2 \; . \tag{49}$$

This procedure is part of the regularization scheme. In the scaling limit, the physical results are independent of the details described in (49). However, it turns out that the definition limits the numerical accuracy for the values of $\Sigma(k^2)$, $Z(k^2)$ for large values of k^2. In order to estimate statistical and systematic numerical errors, we set up a second program, where we solved the Dyson-Schwinger equations (7,8) *after* the loop momentum $k \to k - p$ was shifted. In the second program, one need not to resort to a truncation scheme like that in (49).

From subsection 2.3, we know that the self-energy $\Sigma(k^2)$ decreases like $1/k^2$ up to logarithmic corrections. Close to the numerical cutoff, the self-energy takes values which are 10^{-7} times smaller than the self-energy at zero momentum. In order to extract the slope of the logarithmic decrease (which is related to the quark condensate by (10)), a refinement of the numerical approach is necessary. It turned out to be convenient to introduce the auxiliary variable

$$\sigma(k^2) \;=\; \left(1 \,+\, \frac{k^2}{\Lambda_{QCD}^2}\right) \, \Sigma(k^2) \; . \tag{50}$$

At small values of k^2, $\sigma(k^2)$ essentially coincides with $\Sigma(k^2)$. The advantage is that $\sigma(k^2)$ decreases only logarithmically at asymptotic large values of k^2. To summarize, the second program solves the equivalent set of differential equations, i.e.

$$\begin{aligned}
\sigma(p^2) \;&=\; m \,+\, 4G \int_{|k-p|<\Lambda_I} \frac{d^4k}{(2\pi)^4} \, \frac{\sigma(k^2)}{N(k^2)} \frac{\Lambda_{QCD}^2 + p^2}{\Lambda_{QCD}^2 + k^2} \qquad (51) \\
&+\; 4 \int_{|k-p|>\Lambda_I} \frac{d^4k}{(2\pi)^4} \, \frac{\sigma(k^2)}{N(k^2)} \frac{\Lambda_{QCD}^2 + p^2}{\Lambda_{QCD}^2 + k^2} \, \frac{4\pi\alpha((k-p)^2)}{(k-p)^2} \; , \\
Z(p^2) \;&=\; 1 + \frac{4G}{3} \int_{|k-p|<\Lambda_I} \frac{d^4k}{(2\pi)^4} \, \frac{Z(k^2)}{N(k^2)} \left(3\frac{p\cdot k}{p^2} + 2\frac{(p\cdot k)^2 - p^2k^2}{(k-p)^2} \right) \\
&+\; \frac{4}{3} \int_{|k-p|>\Lambda_I} \frac{d^4k}{(2\pi)^4} \, \frac{Z(k^2)}{N(k^2)} \left(3\frac{p\cdot k}{p^2} + 2\frac{(p\cdot k)^2 - p^2k^2}{(k-p)^2} \right) \\
&\times\; \frac{4\pi\alpha((k-p)^2)}{(k-p)^2} \; , \qquad (52)
\end{aligned}$$

where

$$N(k^2) \;=\; Z^2(k^2)k^2 + \frac{\sigma^2(k^2)}{1 + k^2/\Lambda_{QCD}^2} \; . \tag{53}$$

It turns out that both programs produce practically the same results, which establishes that our results are independent from the regularization scheme. The second program is, however, superior for calculating the quark condensate.

2. The quark condensate

The quark condensate can be extracted from the asymptotic behavior of the quark mass function in (10). For this purpose, we exploit the fact that the function $M(p^2)p^2$ is almost a linear function of $\ln(\ln p^2)$ for sufficiently large values of p^2 (see figure 2). A line fit provides the quark condensate and the numerical estimate of the anomalous dimension D_m. In order to estimate the error of the condensate, we use equation (34), which analytically relates the trace of the quark propagator to the quark condensate. We learn that the error $d_m - D_m$ in the determination of the anomalous dimension implies that we miss the true value for the condensate by a factor

$$\left[\ln \frac{\Lambda_{UV}^2}{\Lambda_{QCD}^2}\right]^{d_m - D_m} \quad . \tag{54}$$

Since we know the correct anomalous dimension analytically ($d_m = 4/9$ from (11) and (15)), equation (54) allows for an estimate of the numerical error, and gives rise to the error bars in figure 4.

3. The critical coupling

In order to extract the critical coupling G_c (see equation (17)), we consider the self-energy (see figure 3)) and the quark condensate (see figure 4), respectively, at small values $G - G_c$. We perform a mean square fit to the 6–8 points which are closest to G_c. For this range of the coupling constant, we expect that the quantities Σ and $\langle\bar{q}q\rangle$ show the critical behavior according

$$\{\Sigma, \langle\bar{q}q\rangle\} \;=\; c_{\Sigma,\langle\bar{q}q\rangle} \left(\frac{G}{G_c} - 1\right)^{\delta_{\Sigma,\langle\bar{q}q\rangle}} \quad . \tag{55}$$

We then perform a mean square fit according (55) to the self-energy and the condensate data points, respectively. This procedure, in particular, results in the critical exponents δ_Σ and $\delta_{\langle\bar{q}q\rangle}$ and in two (nearly identical) values for G_c. The difference in the obtained values for G_c in each case provides an estimate of the numerical error in G_c.

B Asymptotic form of the self-energy

In order to estimate the contribution of the gluon exchange term (second line of (7)), we shift the momentum integration, yielding

$$\Sigma(p^2) \;\approx\; m \;+\; 4\int \frac{d^4k}{(2\pi)^4}\, \frac{\Sigma(k)}{Z^2k^2 + \Sigma^2}\, \frac{4\pi\alpha((p-k)^2)}{(p-k)^2}\theta(|p-k| - \Lambda_I)\;, \tag{56}$$

$$Z(p^2) \;\approx\; 1 \;+\; \frac{4}{3p^2}\int \frac{d^4k}{(2\pi)^4}\;\frac{Z(k)}{Z^2k^2+\Sigma^2}\;\left(2p\cdot k + \mathrm{tr}\,\frac{\not p(\not k-\not p)\not k(\not k-\not p)}{4(p-k)^2}\right) \quad (57)$$
$$\frac{4\pi\alpha((p-k)^2)}{(p-k)^2}\theta(|p-k|-\Lambda_I)\;.$$

We also employ a modified Landau approximation, i.e.

$$\alpha\left((p-k)^2\right)\;\theta\left((p-k)^2-\Lambda_I^2\right)\;\approx\;\alpha\left(\max(p^2,k^2)\right)\;\theta\left(\max(p^2,k^2)-\Lambda_I^2\right)\;. \quad (58)$$

Numerical results confirm that this approximation is valid in the context under considerations of this section. The technical benefit is that we can now explicitly perform the angle integration in (56) and (57). In particular, the angle-integral in (57) corresponds to that of QED in Landau gauge, which is known to be zero [18]. It is therefore consistent to set $Z(p^2)=1$ for the large values of p^2, in agreement with the numerical results (see figure 1). Within the approximation (58) the asymptotic momentum dependence of the mass function $M(p^2)$ coincides with that of the self-energy $\Sigma(p^2)$, i.e.

$$M(p^2)\;\approx\;\Sigma(p^2)\;,\qquad \text{for}\qquad p^2\gg\Sigma^2(0)\;. \quad (59)$$

It is straightforward to evaluate the angle integration in (56), i.e.

$$\Sigma(p^2)\approx m\;+\;\frac{\alpha(p^2)}{\pi p^2}\int_0^{p^2}dk^2\;k^2\;\frac{\Sigma(k^2)}{k^2+\Sigma^2}\;+\;\frac{1}{\pi}\int_{p^2}^{\Lambda_{UV}}dk^2\;\alpha(k^2)\;\frac{\Sigma(k^2)}{k^2+\Sigma^2}\;. \quad (60)$$

where an UV-cutoff Λ_{UV} was introduced, that will be taken to infinity at the end. We will now show that the Ansätze (13) and (16) are self-consistent solutions to (60) at large momentum p^2. First, the case of explicit chiral symmetry breaking is considered. To calculate the first integral at the right hand side of (60), an arbitrary but sufficiently large scale ν was introduced so that the self-energy $\Sigma(p^2)$ can be approximated by (13)) for $p^2\gg\nu^2$, i.e.

$$\frac{\alpha(p^2)}{\pi p^2}\qquad\int_0^{p^2}dk^2\;k^2\;\frac{\Sigma(k^2)}{k^2+\Sigma^2}\;=\;\frac{\alpha(p^2)}{\pi p^2}\int_0^{\nu^2}dk^2\;k^2\;\frac{\Sigma(k^2)}{k^2+\Sigma^2} \quad (61)$$
$$+\quad\frac{\alpha(p^2)}{\pi p^2}\int_{\nu^2}^{p^2}dk^2\;k^2\;\frac{\Sigma(k^2)}{k^2+\Sigma^2}\;=\;\frac{12\kappa}{(33-2N_f)\;\ln^{\alpha+1}p^2/\Lambda_{QCD}^2}$$
$$+\quad\mathcal{O}\left(\frac{\kappa}{\ln^{\alpha+2}p^2/\Lambda_{QCD}^2}\right)\;+\;\mathcal{O}\left(\frac{\nu^2}{p^2\ln p^2/\Lambda_{QCD}^2}\right)\;.$$

The second integral on the right hand side of (60) is

$$\frac{12}{33-2N_f}\qquad\int_{p^2}^{\Lambda_{UV}^2}\frac{du}{u}\frac{\kappa}{\ln^{\alpha+1}u/\Lambda_{QCD}^2}\;= \quad (62)$$
$$\frac{12}{(33-2N_f)\;\alpha}\left[\frac{\kappa}{\ln p^2/\Lambda_{QCD}^2}-\frac{\kappa}{\ln\Lambda_{UV}^2/\Lambda_{QCD}^2}\right]\;.$$

We find that the term (61) is sub-leading at large p^2. Our Ansatz solves (60) for

$$\alpha \;=\; \frac{12}{33-2N_f} \;=\; d_m \;, \qquad \kappa \;=\; m_R(\mu)\left[\ln(\mu^2/\Lambda^2_{QCD})\right]^{d_m} \;, \tag{63}$$

and a bare current mass

$$m(\Lambda_{UV}) \;=\; \frac{m_R(\mu)\left[\ln(\mu^2/\Lambda^2_{QCD})\right]^{d_m}}{\ln^{\alpha}\Lambda^2_{UV}/\Lambda^2_{QCD}} \;. \tag{64}$$

Our goal is now to show that α can be identified with the anomalous dimension of the current mass, and that then the high-energy behavior of the quark mass function as predicted by the operator product expansion (see (10)) is obtained.
In the absence of explicit chiral symmetry, we assume equation (16) to be the correct high momentum behavior of the self-energy $\Sigma(p^2)$. One first estimates

$$\begin{aligned}
&\frac{\alpha(p^2)}{\pi p^2}\int_0^{p^2} dk^2\; k^2\;\frac{\Sigma(k^2)}{k^2+\Sigma^2} \;=\; \frac{\alpha(p^2)}{\pi p^2}\int_0^{\nu^2} dk^2\; k^2\;\frac{\Sigma(k^2)}{k^2+\Sigma^2} \\
&+\frac{\alpha(p^2)}{\pi p^2}\int_{\nu^2}^{p^2} dk^2\; k^2\;\frac{\Sigma(k^2)}{k^2+\Sigma^2} \;=\; d_m\frac{c}{(1-\beta)\;p^2\;\ln^{\beta}p^2/\Lambda^2_{QCD}} \\
&+\mathcal{O}\left(\frac{1}{p^2\ln p^2/\Lambda^2_{QCD}}\right) \;.
\end{aligned} \tag{65}$$

Here β had to be assumed smaller than 1, which will later turn out to be the case. The last term on the right hand side of (60) is

$$\frac{1}{\pi}\int_{p^2}^{\Lambda^2_{UV}} dk^2\;\alpha(k^2)\,\frac{\Sigma(k^2)}{k^2+\Sigma^2} \;=\; \mathcal{O}\left(\frac{1}{p^2\ln^{\beta+1}p^2/\Lambda^2_{QCD}}\right) \;. \tag{66}$$

In contrast to the case of explicit chiral symmetry breaking (62), the contribution of the second term (66) is now sub-leading to the term (65) (provided that $0<\beta<1$). The contribution from the upper bound Λ^2_{UV} in (66) decreases faster than $1/\Lambda^2_{UV}$. We can therefore safely remove the cutoff, i.e. $\Lambda^2_{UV}\to\infty$, since this contribution decreases faster with the regulator than counter-terms. This, in particular, implies that we must have $m_R\equiv 0$, since the contribution from the regulator can not account for the logarithmic decrease with Λ_{UV} of the current mass term. In order the Ansatz (16) to be a solution of the Dyson-Schwinger equation in the asymptotic region (60), one must impose

$$\beta \;=\; 1-d_m \;, \qquad m_R(\Lambda_{QCD})\equiv 0 \;. \tag{67}$$

Note that for three quark flavors $N_f=3$ one finds $\beta=0.555\ldots$ and $0<\beta<1$ as assumed before. Our main observation here is that the Ansatz (16) is the correct asymptotic behavior of the self-energy in the chiral limit, accompanied by the correct anomalous dimensions of the quark condensate as obtained by the operator product expansion (see (10)).

C Pion decay constant and normalization of the BS-vertex

The normalization of the pion BS-vertex in (24) can be derived from the observation that the axial-vector vertex Γ_5^μ contains a pion pole term [29]. With the assumption that this pole term dominates in the chiral limit, we have [15]

$$\vec{\Gamma}_5^\mu(k_+,k_-) \stackrel{\longrightarrow}{p\to 0} \sum_a P^a(k_+,k_-)(\frac{1}{p^2}) \langle 0|\vec{A}_5^\mu|\pi^a(p)\rangle \stackrel{\longrightarrow}{p\to 0} \vec{P}(k_+,k_-) f_\pi \frac{p^\mu}{p^2} , \tag{68}$$

where the arrows indicate the iso-spin vector. Combing this with the Ward identity for the axial vector vertex in the chiral limit

$$p_\mu \vec{\Gamma}_5^\mu(k_+,k_-) \;=\; \frac{\vec{\tau}}{2} \left[S^{-1}(k_+)\gamma_5 + \gamma_5 S^{-1}(k_-)\right] \tag{69}$$

one recovers that the quark self-energy constitutes the BS-vertex in the chiral limit. In addition, (69) provides its proper normalization, i.e.

$$\vec{P}_0(k,0) \;=\; \vec{\tau}\,\gamma_5 \frac{\Sigma_0(k)}{f_\pi} . \tag{70}$$

A particular pion state, e.g. the π^+ which we will consider in the following, is given by

$$P_0^+(k) \;= \frac{1}{\sqrt{2}}\left(P_0^1(k) + iP_0^2(k)\right) = \;\tau^+\,\gamma_5 \frac{\sqrt{2}}{f_\pi}\Sigma_0(k) , \quad \tau^+ = \frac{1}{2}(\tau_1 + i\tau_2) . \tag{71}$$

In order to extract an explicit formula for the pion decay constant f_π, we exploit the fact that the pion electro-magnetic charge is properly normalized to one. For this purpose, we study the electro-magnetic form-factor at zero photon momentum, i.e.

$$\begin{aligned} 2p_\mu F_\pi(p^2,0) \;&=\; \mathrm{tr}\left[\frac{2}{3}\int_k P_0^\dagger(k) S(k_+)\Gamma_\mu(k_+,k_+)S(k_+)P_0(k)S(k_-)\right. && (72)\\ &-\; \left.\frac{1}{3}\int_k P_0^\dagger(k)S(k_+)P_0(k)S(k_-)\Gamma_\mu(k_-,k_-)S(k_-)\right] , && (73)\end{aligned}$$

where $k_\pm = k \pm p/2$, and $\Gamma_\mu(k_-,k_-)$ is the full quark photon vertex. This vertex is unambiguously provided by the differential form of the Ward identity, i.e.

$$\Gamma_\mu(k,k) \;=\; \frac{\partial}{\partial k^\mu} S^{-1}(k) . \tag{74}$$

With the help of this equation, (72) can be cast into

$$2\,p_\mu \;=\; -2\,\mathrm{tr}\left[\frac{2}{3}\int_k P_0^\dagger(k)\frac{\partial S(k_+)}{\partial p^\mu}P_0(k)S(k_-) \;+\frac{1}{3}\int_k P_0^\dagger(k)S(k_+)P_0(k)\frac{\partial S(k_-)}{\partial p^\mu}\right] . \tag{75}$$

Using the decomposition $S(p) = i\not{p}\sigma_V(p^2) + \sigma_S(p^2)$ for the quark-propagator (6), one realizes that both integrals at the right hand side of (75) yield the same value. One therefore finds

$$1 \;=\; -\frac{d}{dp^2}\left(tr \int_k P_0^\dagger(k) S_0(k_+) P_0(k) S_0(k_-) \right)\Big|_{p^2=0} \;. \tag{76}$$

Inserting the BS-vertex (24) in the chiral limit into (76), we finally obtain an explicit expression for the pion decay constant, i.e.

$$\begin{aligned} f_\pi^2 \;&=\; \frac{N_c}{8\pi^2} \int \Sigma_0^2 \Big[-2\sigma_S\sigma_S' + \sigma_V^2 - 2\sigma_V\sigma_V' k^2 - k^2\sigma_S\sigma_S'' \\ &+\; k^2\sigma_S'\sigma_S' - k^4\sigma_V\sigma_V'' + k^4\sigma_V'\sigma_V' \Big] k^2 dk^2 \;, \end{aligned} \tag{77}$$

where the prime denotes the derivative of the function with respect to its argument k^2. This formula was first obtained in [30].

Acknowledgments:
We thank R. Alkofer for valuable comments on the manuscript.

References

[1] F. J. Yndurain, *Quantum Chromodynamics* , Springer Verlag, 1983; P. Pascual and R. Tarrach, *QCD: Renormalization for the Practitioner* (Springer Verlag 1984); J. Collins, *Renormalization* , Cambridge University Press, 1984.

[2] K. Langfeld, L. v. Smekal, H. Reinhardt, Phys. Lett. **B362** (1995) 128.

[3] Ta-Pei Cheng, Ling-Fong Li, *Gauge theory of elementary particle physics* , Oxford-University-Press, NY 1984.

[4] Y. Nambu and G. Jona-Lasinio, Phys. Rev. **124** (1961) 246,255.

[5] C. G. Callan, R. Dashen, D. J. Gross, Phys. Rev. **D17** (1978) 2717, **D19** (1978) 1826; E. V. Shuryak, Nucl. Phys. **B203** (1982) 93, **B302** (1988) 259.

[6] M. B. Halpern, Phys. Rev. **D16** (1977) 1798,3515, M. Schaden, H. Reinhardt, P. A. Amundsen and M. J. Lavelle, Nucl. Phys. **B339** (1990) 595; P. A. Amundsen and M. Schaden, Phys. Lett. **B252** (1990) 265.

[7] H. Reinhardt, Phys. Lett. **B257** (1991) 375, K. Langfeld and M. Schaden, Phys. Lett. **B272** (1991) 100.

[8] C. N. Leung, S. T. Love, W. A. Bardeen, Nucl. Phys. **B273** (1986) 649. W. A. Bardeen, C. N. Leung, S. T. Love, Phys. Rev. Lett. **56** (1986) 1230.

[9] M. Chemtob, K. Langfeld, *Chiral symmetry breaking in strongly coupled scalar QED*, **hep-ph/9506341.**

[10] D. Ebert, H. Reinhardt, Nucl. Phys. **B271** (1986) 188, U. Vogel and W. Weise, Prog. Part. Nucl. Phys. **27** (1991) 195; D. Ebert, H. Reinhardt and M. K. Volkov, Prog. Part. Nucl.Phys. **33** (1994) 1; S. P. Klevansky, Review of Modern Physics **64** (1992) 649.

[11] H. Reinhardt, Phys. Lett. **B244** (1990) 316, R. Alkofer, H. Reinhardt, H. Weigel, Phys. Repts. **265** (1996) 139; R. Alkofer, H. Reinhardt, *Chiral Quark Dynamics*, Lecture notes in physics m33, Springer **1995**.

[12] D. Ebert, T. Feldmann, R. Friedrich, H. Reinhardt, Nucl. Phys. **B434** (1995) 619; D. Ebert, T. Feldmann, C. Kettner, H. Reinhardt, *A Diquark Model for Baryons Containing One Heavy Quark* , **hep-ph/9506298**.

[13] H. Pagels, Phys. Rev. **D15** (1977) 2991; D. Atkinson, P. W. Johnson, Phys. Rev. **D41** (1990) 1661; G. Krein, A. G. Williams, Mod. Phys. Lett. **4a** (1990) 399.

[14] L. v. Smekal, P. A. Amundsen, R. Alkofer, Nucl. Phys. **A529** (1991) 633.

[15] C. D. Roberts, A. G. Williams, Prog. Part. Nucl. Phys. **33** (1994) 477-575.

[16] N. Seiberg and E. Witten, Nucl. Phys. **B426** (1994) 19; Nucl. Phys. **B431** (1994)484.

[17] K. Langfeld and M. Rho, Nucl. Phys. **A596** (1996) 451; K. Langfeld, *Quark confinement in a random background Gross-Neveu model*, Nucl. Phys. **A in press**.

[18] A. Cohen, H. Georgi, Nucl. Phys. **B314** (1989) 7.

[19] V. A. Miransky, K. Yamawaki, Mod. Phys. Lett. **A4** (1989) 129; V. A. Miransky, T. Nonoyama, K. Yamawaki, Mod. Phys. Lett. **A4** (1989) 1409.

[20] V. A. Miransky, M. Tanabashi, K. Yamawaki, Phys. Lett. **B221** (1989) 177; W. A. Bardeen, C. T. Hill, M. Lindner, Phys. Rev. **D41** (1990) 1647;

[21] H. D. Politzer, Nucl. Phys. **B117** (1976) 397, Phys. Lett. **B116** (1982) 171.

[22] V. A. Miransky, *Dynamical symmetry breaking in QFT*, World Scientific 1993.

[23] R. T. Cahill, S. M. Gunner, Mod. Phys. Lett. **A10** (1995) 3051;
R. T. Cahill, S. M. Gunner, **hep-ph/9601319**, contribution to the Joint Japan Australia Workshop, Adelaide, November 1995.

[24] M. R. Frank, C. D. Roberts, Phys. Rev. **C53** (1996) 390.

[25] J. Zinn-Justin, *Quantum Field Theory and Critical Phenomena*, (Clarendon Press, Oxford, 1989).

[26] K. Langfeld, C. Kettner, *The quark condensate in the GMOR relation.* , **hep-ph/9601370**, in press by Mod. Phys. Lett. A.

[27] R. T. Cahill, S. M. Gunner, *The Pion Mass Formula*, **hep-ph/9602240**.

[28] C. D. Roberts, *Electromagnetic Pion From-Factor and Neutral Pion Decay Width*, **hep-ph/9408233** ; R. Alkofer, C. D. Roberts, Phys. Lett. **B369** (1996) 101.

[29] R. Jackiw, K. Johnson, Phys. Rev. **D8** (1973) 2386.

[30] R. Alkofer, A. Bender, C. D. Roberts, Int. J. Mod. Phys. **A10** (1995) 3319.